A Study of the Correlations Between Channel and Traffic Statistics in Multihop Networks

Min Xie and Martin Haenggi, *Senior Member, IEEE*

***Abstract*—This paper investigates the correlations between traffic statistics and channel qualities and their impact on the performance of multihop networks. The physical channel is characterized by the probability p_{s} of successful reception, which depends on the multiple access interference (MAI). Since a node contributes to interference only if it has a nonempty buffer upon being scheduled, the MAI is determined not only by the media-access-control (MAC) scheme but also by the traffic statistics. Therefore, the physical channel performance is intertwined with both the MAC scheme and the traffic statistics. We discuss the autocorrelation in the channels themselves and the cross correlation between the channel and traffic rates and derive closed-form expressions for the network throughput and capacity for m-phase time division multiple access (TDMA) and slotted ALOHA. We also find that, in addition to the traffic rate, the traffic burstiness and correlation have a significant influence on p_{s}. For smooth traffic, even without the MAC control, the traffic correlation could induce optimal spatial reuse like TDMA without the overhead of establishing and maintaining the frame structure. For bursty traffic, we propose an approach that employs a packet dropping policy and takes advantage of the traffic correlation to form a similar natural spacing as for smooth traffic.**

***Index Terms*—Access protocols, fading channels, mobile communication, multiaccess communication, Rayleigh channels, time division multiple access (TDMA).**

I. Introduction

MOBILE multihop networks have a broad range of applications in *ad hoc*, multihop cellular, mesh, and vehicular networks. A characteristic issue in multihop networks is that multiple layers closely interact with one another. Hence, a cross-layer analysis is required. This paper studies the interaction between the physical layer, the MAC layer, and the traffic statistics. The physical channel is characterized by the probability p_{s} of successful reception. In interference-limited networks, p_{s} is determined by the received signal-to-interference ratio (SIR), where the interference is referred to as multiple access interference (MAI) and depends on the multiple access protocol [1]. In the saturation state of the network, i.e., the state where all nodes are always backlogged, the MAI solely depends on the MAC scheme. However, the saturation state could result in infinite backlogs and make networks unstable. Practical networks are nonsaturated. The nonbacklogged nodes do not transmit and interfere when they are scheduled. Then, the MAI is not only MAC-dependent but also coupled with the node buffer occupancy, which depends on the arrival process (traffic) and the service process (channel). In wireless multihop networks, the two processes are both autocorrelated and cross correlated with each other.

The autocorrelation in the arrival processes is caused by the multihop transmissions. Since a flow is usually relayed over several hops, and the arrival is the aggregation of the relayed flows and the local flow generated at the node, the arrival processes to each node are correlated, even if all source flows are independently generated. We refer to this correlation as the traffic correlation, which involves many factors such as the channel quality, the MAC scheme, and the buffer occupancy. The autocorrelation in the service processes and the cross correlation between the arrival and service processes are mainly caused by the MAI. Through a study of these correlations, this paper not only reveals the interaction between the physical layer, the MAC layer, and the traffic statistics but also investigates how the three factors interact with each other and how the correlations affect the network throughput and delay.

A. Previous Work

Most previous cross-layer studies between the physical and MAC layers assumed saturated networks and did not consider the traffic statistics. Toumpis and Goldsmith [2] showed that by combining the MAC scheme with power control, the throughput can be improved. In [3]–[5], the MAI power and the probability p_{s} are explicitly derived for ALOHA and time division multiple access (TDMA) over lognormal and Rayleigh fading channels in saturated networks. In the saturated state, to guarantee stability, a special traffic-generation model is used such that new packets are generated only when the buffer becomes empty. This model is simplified and unrealistic since traffic generation is governed by the application layer and not by the physical or the MAC layer. Practical stable networks cannot be saturated, and the nodes cannot be always backlogged. The accurate calculation of p_{s} should eliminate the impact of the nonbacklogged nodes from the MAI and, thus, involves the traffic characteristics.

The other simplification made in previous work is regarding the traffic correlation. It is usually assumed that the arrivals in the network are independent, which, however, hardly holds in

Manuscript received July 17, 2006; revised November 27, 2006 and February 26, 2007. This work was supported in part by the National Science Foundation under Grant CNS 04-47869 and Grant CCF 05-15012 and in part by the Defence Advanced Research Projects Agency IT-MANET Program under Grant W911NF-07-1-0028. The review of this paper was coordinated by Prof. C. Lin.

M. Xie was with the University of Notre Dame, Notre Dame, IN 46556 USA. She is currently with University College London, London WC1E 6BT, U.K. (e-mail: mxie@nd.edu).

M. Haenggi is with the University of Notre Dame, Notre Dame, IN 46556 USA (e-mail: mhaenggi@nd.edu).

Color versions of one or more of the figures in this paper are available online at http://ieeexplore.ieee.org.

Digital Object Identifier 10.1109/TVT.2007.901063

multihop networks due to the presence of the relayed flows. The node buffer occupancies under correlated and independent flows could be quite different, even in a simple two-node network [6].

The node buffer occupancy is also affected by the service process. The service process depends on both the channel rate and the MAC schemes. In contention-based MAC schemes (ALOHA, CSMA, IEEE 802.11 MAC, etc.) [7], the transmission decision is made only when the node has packets. In contention-free MAC schemes (TDMA, frequency division multiple access, and code division multiple access), the transmission order is predetermined, regardless of the buffers. However, the scheduled nodes with empty buffers certainly do not interfere. The saturation state represents an extreme case that overestimates the cumulated interference and leads to very loose performance bounds. The network may severely underutilize the scarce wireless resources.

Interference is measured using different models. Some proposed MAC schemes are evaluated with an oversimplified circular step-function model, which is often referred to as "disk model" [8], in which the probability $p_{\rm s}$ is either zero or one, purely depending on the distance between the transmitters and the receiver. The transmission is regarded to fail if there are transmissions other than the desired one in the (fixed) disk where the receiver is at the origin. However, in practice, the transmission range is time and location varying. Moreover, with a high SIR, even if there is nonzero interference, the node can recover the date, which is referred to as capture property of wireless channels. This property is characterized by the more practical "physical" or "capture model" [3], [4], in which $p_{\rm s}$ is a function of the received SIR. In this paper, we use the capture model.

TDMA [9] and ALOHA [10] are two typical MAC schemes. The former schedules the optimal transmission order and achieves high throughput in heavy traffic. In multihop networks, TDMA not only favors spatial reuse but also provides fast forwarding of packets [11], [12]. However, TDMA is not practical in many mobile multihop networks. The latter is simple and practical but has low throughput for heavy traffic since the random and independent transmission pattern unavoidably causes collisions. Many wireless MAC schemes seek a good balance between the TDMA and the ALOHA. For example, in the reservation-based MAC schemes (MACA [13], IEEE 802.11 MAC, and DBTMA [14]), control and data packets are transmitted on two separate channels. Nodes compete for the control channel in an ALOHA-based fashion for resource reservation, while the successful nodes transmit on the data channel in a TDMA fashion.

However, most of the current MAC schemes are designed for single-hop networks and do not result in optimum transmission patterns in multihop networks [7], [15]. In [16], a multihop TDMA-based reservation MAC protocol is developed for constant-bit-rate (CBR) traffic; the multihop network is partitioned into clusters, each of which is assigned a distinct frame. Collisions are avoided, but spatial reuse is excluded; therefore, the scheme is not scalable. In [17] and [18], spatial reuse is exploited, but the channel is characterized by the disk model. Saligrama and Starobinski [19] discussed the correlation in the channels inherited from the multihop topology for a two-node network. The channel quality of the downstream node is worse with the upstream node transmission than with the upstream node idle. However, the correlation is simply expressed by a predetermined constant, whose calculation is not specified in [19]. Little attention has been paid to other correlations incurred by the multihop topology, particularly the traffic correlation.

B. Our Contributions

Our main contribution is the investigation of the correlations in mobile multihop networks and their impact on the network performance. Three types of correlations are studied, namely, the autocorrelation in channels, the cross correlation between traffic and channels, and the traffic correlation, through the node buffer occupancy. Since the node busy probability is MAC- and traffic-dependent, we consider two typical MAC schemes, namely, the m-phase TDMA and the slotted ALOHA, and three frequently used traffic models, namely, CBR for voice applications, ON–OFF for data applications, and memoryless Bernoulli processes. Closed-form expressions for the network throughput and capacity are derived. Simulation results are provided to compare $p_{\rm s}$ for different MAC schemes and traffic models.

Our study shows that the traffic correlation plays a distinct role in ALOHA. Counterintuitively, for smooth traffic like CBR and light bursty ON–OFF traffic, increasing the access probability to have more nodes that transmit simultaneously does not necessarily degenerate the channel performance, as expected. Instead, the traffic correlation induces optimal spatial reuse in the form of an almost equal spacing between the transmitting nodes so that the throughput is enhanced. For bursty traffic, with a simple packet dropping policy, a similar spacing is induced as for smooth traffic. Then, we analyze the corresponding throughput and packet loss rate, which provides insight on how to achieve a tradeoff between reliability, throughput, and delay.

The rest of this paper is organized as follows. Section II presents the calculation of $p_{\rm s}$ over Rayleigh fading channels and reveals its interaction with the traffic statistics and the MAC schemes. The impact of the correlations on TDMA and ALOHA is studied in Sections III and IV, respectively. In Section V, the performance of networks with non-CBR traffic is analyzed when a packet dropping policy is employed. Concluding remarks are provided in Section VI.

II. Interaction Between Channel, MAC, and Traffic

In certain wireless networks such as vehicular or sensor networks, the topology is quite likely to be regular, like a square grid [Fig. 1(a)] or a regular line [Fig. 1(b)]. Small changes in the distances between nodes are overshadowed by fading. Hence, it is reasonable to assume fixed distances when the channel is modeled as block fading. The transmission is successful with probability $p_{\rm s}$ [20], and we assume immediate feedback on transmission success. To guarantee 100% reliability, failed

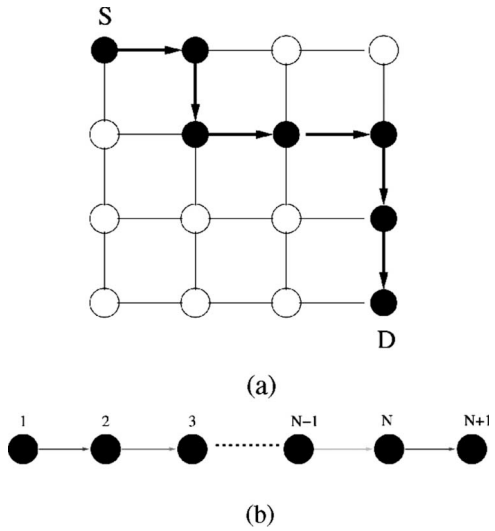

Fig. 1. Regular wireless multihop networks. (a) Manhattan street network. (b) Vehicular line network.

packets will be retransmitted until being correctly received. The time is slotted to one packet transmission duration.

The multihop network [Fig. 1(b)] is composed of N nodes. Denote node i by n_i. Each node independently generates a flow $s_i(t)$ of fixed-length packets with an average rate r_i in packets per second. The arrival to n_i is denoted as $a_i(t)$, which is an aggregation of the relayed flows and the local flow. The arrival rate is $\lambda_i = \sum_{k\in\mathcal{R}_i} r_k$, where $\mathcal{R}_i$ is the set of source nodes whose flows traverse n_i. The network throughput and capacity are defined as follows.

Definition 2.1: The network throughput $\lambda_{\max}$ is the maximum arrival rate that can be accommodated by the network for a given MAC scheme with a specific MAC parameter.

Definition 2.2: The network capacity $\lambda_{\rm C}$ is the maximum arrival rate that can be achieved for a given family of MAC schemes, i.e., maximized over the parameters of that family. Hence, the throughput depends on the MAC parameter (e.g., the access probability p_m in ALOHA or the reuse parameter m in the m-phase TDMA), while the capacity $\lambda_{\rm C} = \max\{\lambda_{\max}\}$ is obtained by maximizing $\lambda_{\max}$ over the MAC parameter.

Assume equal distances between neighboring nodes and equal transmit powers P. Using the shortest path first routing protocol, the receiver of n_i is n_{i+1}. Given a path loss exponent α, in Rayleigh fading channels, the received power is exponentially distributed with mean $Pd_i^{-\alpha}$, where d_i is the distance between n_i and its receiver. For interference-limited networks such as vehicular networks, the transmit energy consumption is not critical so that the noise power can be ignored. The transmission is successful if the received SIR is greater than a threshold Θ, which is determined by the communication hardware and the modulation and coding scheme. According to Mathar and Mattfeldt [4], and Haenggi [5], the success probability $p_{s,i}$ for n_i is

$$p_{s,i} = \mathbb{P}\{\text{SIR}_i > \Theta\} = \prod_{k\in\mathbb{I}_i}\left(1 - \frac{p_t(k,i)}{1+\left(\frac{d_{k,i}}{d_i}\right)^{\alpha}/\Theta}\right) \quad (1)$$

where $\mathbb{I}_i$ is the interference set consisting of all potential interferers of n_i, and $d_{k,i}$ is the distance between the interferer n_k and the receiver of n_i. When n_i is transmitting, the interferer n_k transmits with the effective transmit probability $p_t(k,i) \triangleq p_{m,k}p_{\rm b}(k,i)$, where $p_{m,k}$ is the MAC-dependent access probability of n_k, and $p_{\rm b}(k,i) \le 1$ is the conditional busy probability of n_k, given that n_i is transmitting. As a conditional probability, $p_{\rm b}(k,i)$ measures the correlation between n_k and n_i.

In the saturated networks, $p_{\rm b}(k,i) \equiv 1$, and $p_t(k,i)$ is simplified to $p_t(k,i) = p_{m,k}$ so that the correlation between n_k and n_i can be ignored. The saturation state is a special case which not only eliminates the correlation between n_k and n_i but also overestimates the cumulated interference and leads to a very conservative $p_{s,i}$, particularly when $p_{\rm b}(k,i) \ll 1$. In practice, the simplification $p_{\rm b}(k,i) \equiv 1$ is not appropriate.

In order to explain how n_i and n_k are correlated, we consider a simple two-node tandem network in Fig. 2, where $i = 1$, and $k = 2$. The channel can be regarded as a time-varying demultiplexer that forwards the packets to the following node with probability $p_{s,i}(t)$ while returning the packets to the buffer for retransmission with probability $1 - p_{s,i}(t)$. Given the MAC control parameter $p_{m,i}$, at any time slot, the busy node successfully transmits a packet with probability $p_{m,i}p_{s,i}(t)$. Then, the buffer occupancy $B_i(t)$ is $B_i(t) = B_i(t-1) + a_i(t) - \mathbf{1}_{\{B_i(t-1)\}}$ with probability $p_{m,i}p_{s,i}(t)$. Otherwise, $B_i(t) = B_i(t-1) + a_i(t)$. Here, $\mathbf{1}_{\{B_i(t-1)\}} = 1$ if $B_i(t-1) > 0$; otherwise, $\mathbf{1}_{\{B_i(t-1)\}} = 0$. The arrival process $a_i(t)$ is composed of two parts, namely, the local flow $s_i(t)$ and the relayed flow $d_{i-1}(t)$, which is the output of n_{i-1}. The failed packets are directed to the buffer head and, thus, do not change the buffer size. The service rates $p_{s,1}(t)$ and $p_{s,2}(t)$ synchronously change. For instance, if $p_{s,k}(t)$ increases, the buffer $B_k(t)$ will be cleared more quickly, and $p_{\rm b}(k,i)$ will decrease. Based on (1), a decreasing $p_{\rm b}(k,i)$ results in an increase of $p_{s,i}$ and vice versa. This positive correlation is very similar to the self-clocking property in TCP [21]. Therefore, the demultiplexers of n_k and n_i are connected by a self-clocking controller in Fig. 2. Similarly, an increase of the arrival rate λ_k [or $a_k(t)$] will result in an increase of $B_k(t)$. Then, $p_{\rm b}(k,i)$ increases, and in turn, $p_{s,i}$ decreases.

In addition to the autocorrelation in the channel qualities $p_{s,i}(t)$ and the cross correlation between the arrival $a_i(t)$ (or λ_i) and channel qualities $p_{s,i}(t)$, there is another correlation in the network, which is induced by the multihop topology. The arrivals $a_i(t)$ and $a_k(t) = s_k(t) + d_i(t)$ are correlated through $d_i(t)$, which originates from $a_i(t)$. The correlation level depends on the similarity between $d_i(t)$ and $a_i(t)$ and the fraction of $d_i(t)$ in the arrival process $a_k(t)$.

For a tractable analysis, we consider two extreme cases, namely, local traffic only and relayed traffic only. In the first case, there is no relayed traffic, so $d_i(t) \equiv 0$, $a_k(t) = s_k(t)$, and $\lambda_k = r_k$, and the arrival processes are independent. In the second case, there is no local traffic (except for the single source node), so $s_k(t) \equiv 0 (k \neq 1)$. In 1-D networks [Figs. 1(b) and 2], $a_1(t) = s_1(t)$, $a_k(t) = d_i(t)$, and $\lambda_k = r_1$, and the arrival processes are completely correlated. The two cases provide upper and lower bounds for other correlation levels. For a fair comparison of the two cases, we set the rate $r_i = \lambda$.

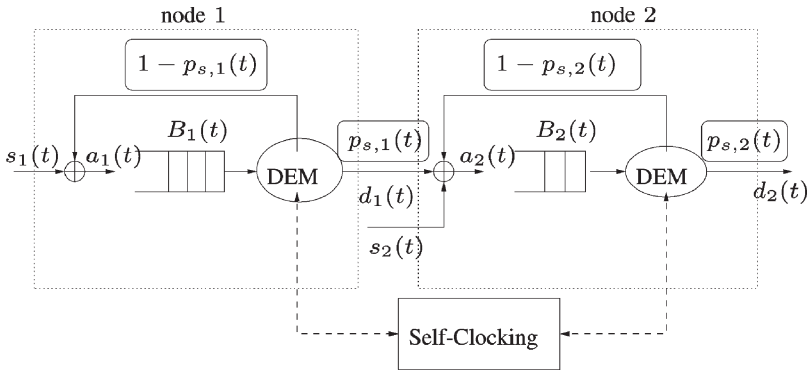

Fig. 2. Two-node tandem network. Each server directs the traffic flow to its downstream neighbor with probability $p_{s,i}(t)$ and returns the packets to the head of the buffer with probability $1-p_{s,i}(t)$. The servers are connected by a self-clocking controller.

The buffer occupancy $B_i(t)$ and the corresponding busy probability $p_{\rm b}(k,i)$ are affected by the arrival processes and the channel qualities. Since the channel qualities cannot directly be controlled, we explore how the traffic flow $s_i(t)$ affects the conditional probability $p_{\rm b}(k,i)$. For comparison, we also consider the unconditional busy probability ρ_k (the traffic intensity), which is defined by queueing theory as the ratio of the arrival rate to the service rate. The impact of the traffic statistics is reflected by the ratio of $p_{\rm b}(k,i)$ to ρ_k in the presence of the aforementioned correlations.

1) **Arrival rate**, which determines the traffic intensity. If $\rho_k \to 1$, n_k becomes saturated and is always busy whenever n_i is transmitting, i.e., $p_{\rm b}(k,i) \to \rho_k \approx 1$.
2) **Traffic burstiness** [22]. In Fig. 2, if packets arrive in batches at n_1, the buffer $B_1(t)$ is nonempty after one packet is delivered to n_2. At the following time, neither $B_1(t)$ nor $B_2(t)$ is empty even if n_2 itself does not generate packets, implying a high $p_{\rm b}(k,i)$. On the other hand, if the packet arrivals are separated by a nonzero interval, this phenomenon rarely happens since $B_1(t)$ becomes empty after the packet is delivered to n_2. Therefore, $p_{\rm b}(k,i)$ is small.

To distinguish the impact of traffic burstiness, we consider three typical traffic models, namely, CBR, ON–OFF, and Bernoulli. In CBR, the packet interarrival time is a constant $R=1/\lambda$. In ON–OFF, the arrival process is modulated by a two-state Markov chain that alternates between ON (1) and OFF (0) states. A packet is generated only when the Markov chain is in state ON. The transition probabilities between ON and OFF are a_{01} and a_{10}, respectively. This model generates a stream of correlated bursts and silent periods, both of which are geometrically distributed in length with a mean burst of length $1/a_{10}$ and average rate $r=a_{01}/(a_{10}+a_{01})$. Bernoulli is a special ON–OFF model with $a_{01}+a_{10}=1$ so that the generated burst and silent periods are independent.

Because of the correlation between $B_i(t)$ and $B_k(t)$, generally $p_{\rm b}(k,i) \neq \rho_k$. However, if the correlation decreases, then $p_{\rm b}(k,i) \approx \rho_k$. In the 1-D network, the set of tandem nodes can be regarded as a Markov chain. Intuitively, the correlation will diminish if n_k and n_i are far away from each other. Since the distance between the transmitter and its interferers is determined by the MAC scheme, we investigate two typical MAC schemes, namely, the m-phase TDMA and the slotted ALOHA, in the following sections.

III. m-PHASE TDMA

In the m-phase TDMA [9], every node is allocated to transmit once in m time slots, which is defined as one frame. In multihop networks like the 1-D network [Fig. 1(b)], the nodes that are m hops apart can transmit simultaneously to achieve spatial reuse. Then, the interferers are $lm (l=1,2,\ldots)$ hops away from the transmitter n_i and have access probability $p_{m,k}=1$. The distance from the interferer n_k to the receiver is $d_{k,i}/d_i = lm+1$ if n_k is on the left side of n_{i+1}, which is referred to as a left interferer, and $d_{k,i}/d_i = lm-1$ if n_k is on the right side of n_{i+1}, which is referred to as a right interferer. With m chosen appropriately, the interferers $\{n_k\}$ and transmitter n_i are far away. Then, it is reasonable to approximate $p_{\rm b}(k,i) \approx \rho_k$. In [23], at the frame level, ρ_k is derived as $\rho_k = m\lambda/p_{s,k}$, in which the arrival rate λ is multiplied by a factor m to account for the packet accumulation in one frame of m slots. Based on (1), we have

$$p_{s,i} = \prod_{k\in\mathbb{I}_i} \left(1 - \frac{m\lambda}{p_{s,k}\left(1+(lm\pm 1)^{\alpha}/\Theta\right)}\right) \tag{2}$$

where $\mathbb{I}_i = \{k | (k \bmod m) = (i \bmod m)\}$, and $d_k/d_i = lm \pm 1$. The positive correlation in the channel qualities $\{p_{s,i}, p_{s,k}\}$ and the negative correlation between the channel quality $p_{s,i}$ and the arrival rate λ are explicitly revealed in (2), which permits the calculation of the corresponding network throughput and capacity.

A. Network Throughput and Capacity

The network throughput is determined by the max-flow mincut. Assume that the worst channel quality is $p_{\rm sL}$. The network traffic distribution can be classified into heterogeneous and homogeneous, which is distinguished by whether the arrival rates at each node are identical or not. For the homogeneous traffic distribution, $\lambda_i = \lambda_k = \lambda$, and the network throughput and capacity are calculated when $\lambda = \max_i\{\lambda_i\}$. Thus, $p_{\rm sL}$ occurs at the center nodes that have approximately the same

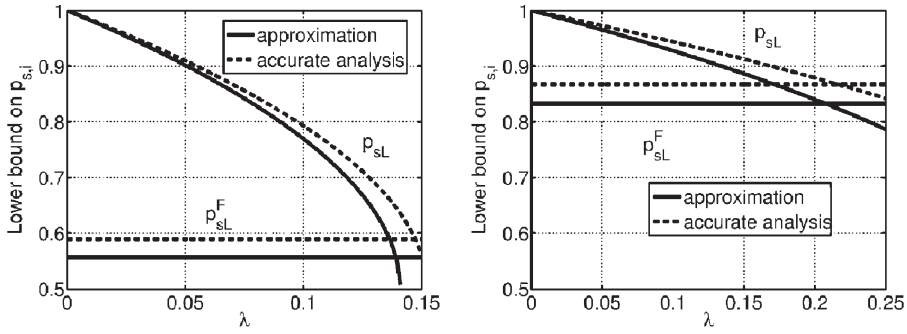

Fig. 3. Comparison of the worst channel quality $p_{\rm sL}$ in the nonsaturated (9) and saturated (10) TDMA line networks with $\Theta = 10$ and $m = 4$. (a) $\alpha = 3$. (b) $\alpha = 4$.

number of right and left interferers, which is denoted by K, where

$$K = \left\lceil \frac{\lfloor \frac{N}{m} \rfloor}{2} \right\rceil - 1. \tag{3}$$

By replacing $p_{s,k} \geq p_{\rm sL}$ into (2), we approximate $p_{\rm sL}$ as follows:

$$\begin{aligned} p_{\rm sL} &\leq \prod_{l\in\mathbb{I}} \left(1 - \frac{m\lambda}{p_{\rm sL}(1+l^\alpha/\Theta)}\right) \\ &\approx 1 - \frac{m\lambda}{p_{\rm sL}} \sum_{l\in\mathbb{I}} \frac{1}{1+l^\alpha/\Theta} \qquad (4) \\ &\lessapprox 1 - \frac{2m\lambda}{p_{\rm sL}} \sum_{l=1}^{K} \frac{1}{1+(lm)^\alpha/\Theta} \qquad (5) \\ &\approx 1 - \frac{2m\lambda}{p_{\rm sL}} \underbrace{\int_{0.5}^{K+0.5} \frac{\Theta}{\Theta+(mx)^\alpha} dx}_{g(m,\Theta,\alpha)} \qquad (6) \end{aligned}$$

where $\mathbb{I} = \{lm+1\}_{l=1}^{K} \bigcup \{lm-1\}_{l=1}^{K}$. In practice, $\Theta \approx 10$ dB, which guarantees $1/(1+(lm\pm 1)^\alpha/\Theta) \ll 1$ and allows us to approximate the product by the sum in (4) [24]. The approximation in (5) uses the convexity of the function $1/(1+x^\alpha/\Theta)$. Since $m^{-\alpha}$ is very small, the sum is approximated by an integral $g(m,\Theta,\alpha)$. For integer α, there exists a closed-form solution. For other values, it can numerically be calculated.

For heterogeneous traffic distribution, $\lambda_i \neq \lambda_j$. A simple example is that every node generates a traffic flow of identical rate $r_i \equiv r$. In the line network, $\lambda_i = ir$, and $\lambda = Nr$. Let L denote the index of the node where $p_{\rm sL}$ occurs. Then

$$L = Km + \text{Rem}\left(\frac{N}{m}\right), \qquad N = L + (K-1)m.$$

A similar calculation as in (6) yields the upper bound (replacing λ by $(L-lm)r$ and $(L+lm)r$ for the distance $lm+1$ and $lm-1$, respectively)

$$\begin{aligned} p_{\rm sL} &\lessapprox 1 - \frac{m\lambda}{p_{\rm sL}} \sum_{l=1}^{K} \frac{1}{1+(lm)^\alpha/\Theta} \\ &\approx 1 - \frac{m\lambda}{p_{\rm sL}} g(m,\Theta,\alpha). \qquad (7) \end{aligned}$$

Apparently, the obtained $p_{\rm sL}$ is greater than that obtained for the homogeneous traffic distribution. Since the network throughput and capacity are determined by the worst-case scenario, they are studied based on the homogeneous traffic distribution (6).

Note that, in (6), $g(m,\Theta,\alpha) \geq 0$ monotonically decreases with m and α, and increases with Θ. Rewrite (6) as a quadratic equation of $p_{\rm sL}$, and solve $p_{\rm sL}$ as

$$p_{\rm sL} \approx \frac{1}{2}\left(1 \pm \sqrt{1 - 8m\lambda g(m,\Theta,\alpha)}\right). \tag{8}$$

A meaningful $p_{\rm sL}$ should satisfy $p_{\rm sL} > 0.5$. Therefore, we eliminate the solution with the minus sign in (8). To obtain real solutions for $p_{\rm sL}$, $8m\lambda g(m,\Theta,\alpha) < 1$, which can be used as a constraint to design the network altogether with the fundamental stability condition $\rho = m\lambda/p_{\rm sL} < 1$. In particular, for $\alpha = 2$, the integral can be expressed in closed form. For $K \to \infty$, it is simplified to

$$p_{\rm sL} \approx \frac{1}{2} + \sqrt{\frac{1}{4} - 2\sqrt{\Theta}\lambda\left(\frac{\pi}{2} - \arctan\left(\frac{m}{2\sqrt{\Theta}}\right)\right)}. \tag{9}$$

Note that if $\Theta = 0$ or $m \to \infty$, $g(m,\Theta,\alpha) = 0$ and, thus, $p_{\rm sL} = 1$, as expected. The dependence of $p_{\rm sL}$ on the arrival rate λ and the MAC parameter m is clearly displayed in (8) and (9). The inclusion of λ distinguishes our analysis (8) from previous work [3]–[5] for saturated networks. As a comparison, consider the worst channel quality in saturated networks and denote it by $p_{\rm sL}^{\rm F}$ for full load. By plugging $p_{\rm b}(k,i) \equiv 1$ into (2), we have

$$p_{\rm sL}^{\rm F} \approx 1 - 2g(m,\Theta,\alpha). \tag{10}$$

Fig. 3 compares $p_{\rm sL}$ and $p_{\rm sL}^{\rm F}$, for $\Theta = 10,$ and $m = 4$. Apparently, $p_{\rm sL}^{\rm F}$ is independent of λ and is a constant for fixed Θ and α. The channel quality in the nonsaturated state is better than in the saturated state, particularly when the arrival rate is low. Accordingly, the Quality of Service (QoS), like buffer

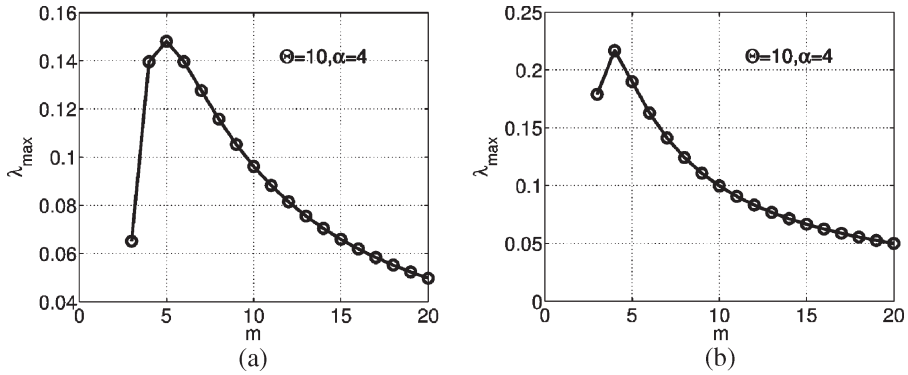

Fig. 4. Network throughput $\lambda_{\max}$ as a function of TDMA parameter m in a line network with $\Theta = 10$. (a) $\alpha = 3$. (b) $\alpha = 4$.

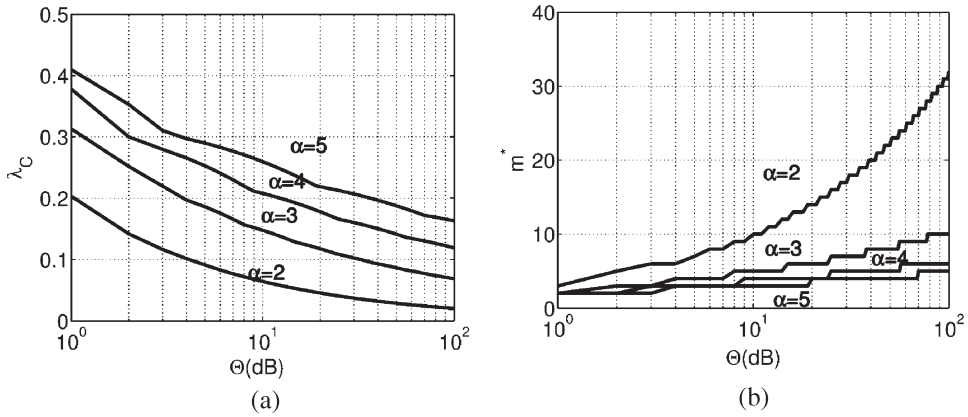

Fig. 5. Network capacity $\lambda_{\rm C}$ of TDMA line networks. (a) $\lambda_{\rm C}$. (b) m^*.

occupancy and packet delay, can more easily be guaranteed than in the saturated state.

The network throughput is derived from the stability condition, i.e., the traffic intensity should be smaller than one ($m\lambda/p_{\rm sL} < 1$). Based on (8), λ should satisfy the following condition:

$$2m\lambda < 1 + \sqrt{1 - 8m\lambda g(m, \Theta, \alpha)}. \tag{11}$$

The maximum rate $\lambda_{\max}$ is

$$\lambda_{\max} = \frac{1 - 2g(m, \Theta, \alpha)}{m}. \tag{12}$$

Numerical results (Fig. 4, where $\Theta = 10$) show that $\lambda_{\max}$ is a concave function of m. Increasing m will decrease the potential interference and improve the channel capacity $p_{\rm sL}$. However, it also reduces spatial reuse and potentially decreases the network throughput. There is a tradeoff, and our analysis provides the optimum value of m to achieve the best tradeoff.

If $\lambda = \lambda_{\max}$, the network will be saturated. In other words, $\lambda_{\max}$ can be calculated by directly applying $p_{\rm sL}^{\rm F}$ (10) for the saturated network to $m\lambda/p_{\rm sL}^{\rm F} < 1$. Since $\lambda_{\max}$ is concave with respect to m, the network capacity $\lambda_{\rm C} = \max_m\{\lambda_{\max}\}$ is obtained by differentiating $\lambda_{\max}$ over m and equating to zero

$$1 - 2g(m, \Theta, \alpha) + 2mg'_m(m, \Theta, \alpha) = 0 \tag{13}$$

we obtain the optimum value $m_{\rm opt} \in \mathbb{R}$ that achieves $\lambda_{\rm C}$. In practice, the optimum value $m^* \in \mathbb{N}$ should be integer, so $m^* = \lceil m_{\rm opt} \rfloor$. Based on (12)

$$\lambda_{\rm C} = \frac{1 - 2g(m^*, \Theta, \alpha)}{m^*} = -2g'_m(m^*, \Theta, \alpha) \le \frac{1}{m^*}. \tag{14}$$

Since $g(m, \Theta, \alpha)$ is nonnegative, the network capacity cannot exceed $1/m^*$. For instance, given that $\Theta = 10$ and $\alpha = 4$, Fig. 4(b) shows that $m^* = 4$. In Fig. 5, it is confirmed that $\lambda_{\rm C} \approx 0.2 < 1/m^*$. The capacity $\lambda_{\rm C}$ is monotonically decreasing with Θ because a higher SIR threshold Θ restricts spatial reuse and, thus, results in lower capacity.

B. Simulation Results

Throughout this paper, simulation results were obtained using MATLAB for the line network [Fig. 1(b)] with $N = 15$ nodes. All channels are subject to block Rayleigh fading. Path loss exponents α range between two and five. Arrival rates are set to be λ in packets per second. Three traffic models, namely, CBR, ON–OFF, and Bernoulli, are simulated.

In TDMA, the correlation between n_i and its interferer n_k is small enough to be negligible if m is large, for example, $m > 4$. Then, it is reasonable to approximate $p_{\rm b}(k, i) \approx \rho_k$. The traffic burstiness and correlation mainly affect $p_{\rm b}(k, i)$, which, if being approximated by ρ_k, will be dependent only on the traffic rate. Consequently, it is expected that, with an increasing m, the

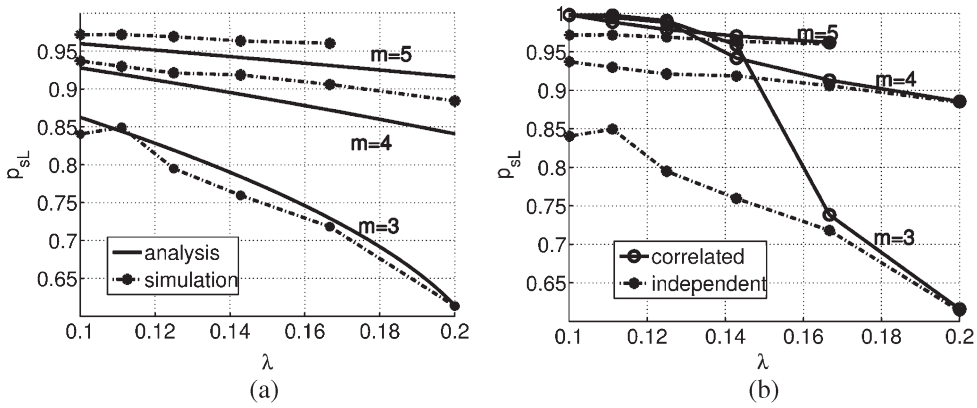

Fig. 6. Channel quality p_{sL} in TDMA networks with CBR traffic and $\alpha = 4$, $\Theta = 10$. (a) Comparison of the analysis and simulations. (b) Comparison of simulated p_{sL} for independent and correlated traffic flows.

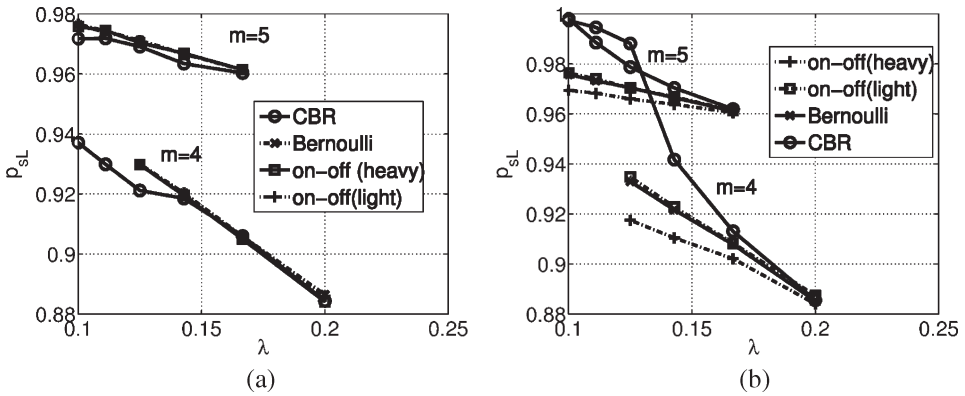

Fig. 7. Impact of traffic burstiness in TDMA networks with $\alpha = 4$ and $\Theta = 10$. (a) Independent traffic flows. (b) Dependent traffic flows.

traffic burstiness and correlation would cause small difference in the channel qualities.

First, Fig. 6(b) confirms that the impact of the traffic correlation does become negligible as m increases. The channels behave similarly, regardless of whether the traffic flows are correlated or independent. Second, in Fig. 7, we can see that traffic burstiness has almost no influence on p_{sL} when the traffic flows are independent. Even though there exists a difference in p_{sL} when traffic flows are correlated, it is less visible with larger m (e.g., $m = 5$). Therefore, the approximation $p_{\mathrm{b}}(k,i) \approx \rho_k$ is quite tight for the analysis of p_{sL}, throughput $\lambda_{\max}$, and capacity λ_{C}. As a matter of fact, Fig. 6(a) verifies that our analysis of p_{sL} (8) is accurate when the traffic flows are independent.

If m is small, the correlation between n_k and n_i cannot be ignored, and the channels behave differently under different models, particularly with correlated traffic. For instance, with correlated flows, in Fig. 6(a) with $m = 3$, the channel quality p_{sL} is substantially improved when traffic is light, for example, $\lambda < 0.15$. Moreover, the impact of traffic burstiness becomes more visible [Fig. 7(b)]. Here, light and heavy bursty ON–OFF processes are defined based on the burst size. Set $1/(1-\lambda)$ (the burst size of Bernoulli traffic) as the standard burst size. Light ON–OFF traffic has a burst size of $(1/(1-\lambda) - (1-\lambda))/2$, while heavy ON–OFF traffic has a burst size of $\lambda/2$. More bursty traffic results in a higher $p_{\mathrm{b}}(k,i)$ and a lower channel quality p_{sL} than smooth traffic [Fig. 7(b)]: the heavier the burstiness, the worse the channel.

Note that the impact of traffic burstiness and correlation is overshadowed by the arrival rate. When the rate λ increases, the channel quality p_{sL} decreases to the same value, regardless of traffic burstiness and correlations. In summary, the correlation between two nodes n_k and n_i depends on four factors in decreasing order of relevance: 1) distance m between n_k and n_i; 2) traffic rate λ; 3) traffic correlation; and 4) traffic burstiness.

IV. Slotted ALOHA

In ALOHA [10], each node n_i independently transmits with access probability $p_{m,i}$ when it has packets. For simplicity, we assume that $p_{m,i} = p_m$ throughout this section. ALOHA with $p_m = 1$ is a special case of TDMA with $m = 1$. Therefore, the interference set $\mathbb{I}_i = \{k | k \neq i\}$ includes the very close neighbors of transmitter n_i, e.g., n_{i+1} and n_{i-1}. The distance between the transmitter and the interferers is too small to neglect the correlation between them as in TDMA. It is quite difficult to derive the correlations. Therefore, ALOHA is studied through simulation results.

In TDMA, we have proved that the network throughput and capacity can be calculated as if the network were in the

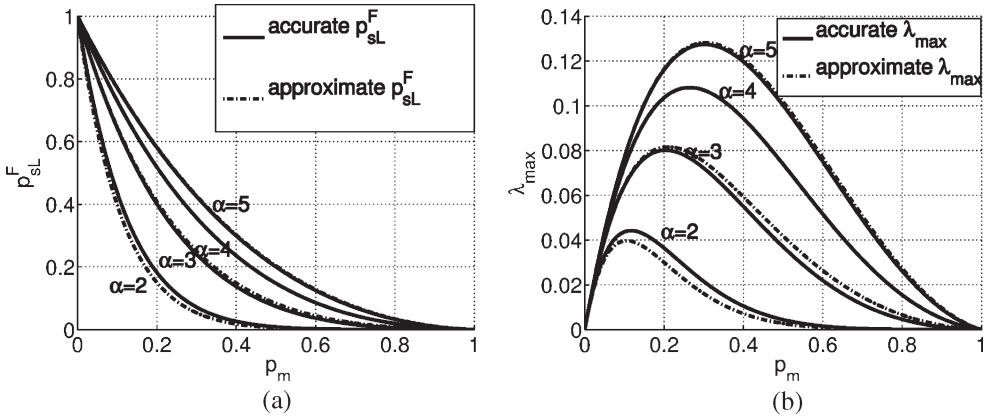

Fig. 8. Network throughput and capacity in ALOHA networks. (a) Lower bound $p_{\mathrm{sL}}^{\mathrm{F}}$ on $p_{s,i}$ for $\Theta = 10$. (b) Network throughput $\lambda_{\max}$.

saturated state. In other words, we can use $p_{\mathrm{b}}(k,i) \equiv 1$ to calculate $\lambda_{\max}$ and λ_{C}.

A. Network Throughput and Capacity in ALOHA

Like in TDMA, in ALOHA line networks [Fig. 1(b)], the bottleneck occurs at the center nodes that have approximately the same number of right and left interferers. The difference lies in that the desired receiver is also a potential interferer, i.e., $d_{k,i}/d_i = 0, 1, 2, \ldots$. In the saturated state, $p_t(k,i) = p_m$. From (1), we obtain

$$p_{\mathrm{sL}}^{\mathrm{F}} \leq (1-p_m)\left(1-\frac{p_m}{1+1/\Theta}\right)\left(\underbrace{\prod_{k=2}^{\infty}\left(1-\frac{p_m}{1+k^{\alpha}/\Theta}\right)}_{h(p_m,\Theta,\alpha)}\right)^2. \tag{15}$$

Like in [25], for small p_m, $\log(1-p_m/(1+k^{\alpha}/\Theta)) \lessapprox -p_m/(1+k^{\alpha}/\Theta)$, which leads to $h(m,\Theta,\alpha) \approx e^{-p_m/\sigma}$, where

$$\sigma^{-1} = \sum_{k=2}^{\infty}\frac{1}{1+k^{\alpha}/\Theta}. \tag{16}$$

In particular, for $\alpha = 2$ and $\alpha = 4$, $h(m,\Theta,\alpha)$ is further simplified to [25]

$$h(m,\Theta,\alpha)\left(1-\frac{p_m}{1+1/\Theta}\right) = \begin{cases} \dfrac{e^{\sqrt{2}y_1}}{\sqrt{1-p_m}e^{\sqrt{2}y_2}}, & \alpha = 2 \\ \dfrac{\cosh^2(y_1)-\cos^2(y_1)}{\sqrt{1-p_m}\left(\cosh^2(y_2)-\cos^2(y_2)\right)}, & \alpha = 4 \end{cases}$$

where $y_1 := \pi\sqrt[\alpha]{\Theta(1-p_m)}/\sqrt{2}$, and $y_2 := \pi\sqrt[\alpha]{\Theta}/\sqrt{2}$. Fig. 8(a) verifies the accuracy of the approximate $g(p_m,\Theta,\alpha)$ in the calculation of $p_{\mathrm{sL}}^{\mathrm{F}}$ when $\alpha > 2$. Using the same technique as in TDMA, i.e., $\rho = \lambda/(p_m p_{\mathrm{sL}}^{\mathrm{F}}) < 1$ [26], we obtain the network throughput $\lambda_{\max}$ as follows:

$$\lambda_{\max} \lessapprox p_m(1-p_m)\left(1-\frac{p_m}{1+1/\Theta}\right)e^{-p_m/\sigma} \tag{17}$$

which is shown in Fig. 8(b). Like in TDMA, $\lambda_{\max}$ is concave with respect to the MAC parameter p_m. In a saturated ALOHA network, if all nodes transmit independently, a higher access probability p_m allows more nodes to transmit simultaneously, which causes more severe interference. On the other hand, a p_m that is too small unnecessarily holds the packets in the buffer for a longer time, which reduces the network throughput. Our analysis presents the optimum p_m^* to achieve the best tradeoff. The capacity λ_{C} is obtained by differentiating $\log(\lambda_{\max}) = \log(p_m) + \log(1-p_m) + \log(1-p_m/(1+1/\Theta)) - p_m/\sigma$ with respect to p_m. The optimal value p_m^* achieves the capacity and is a root to the following polynomial:

$$f(p_m) = c_0 p_m^3 + c_1 p_m^2 + c_2 p_m + c_3 \tag{18}$$

where

$$\begin{cases} c_0 = 2\Theta\sigma^{-1}, & c_1 = -(2\sigma^{-1} + 3\Theta + 4\Theta\sigma^{-1}) \\ c_3 = -(1+\Theta), & c_2 = 2(1 + 2\Theta + \sigma^{-1} + \Theta\sigma^{-1}). \end{cases}$$

Fig. 9(a) shows p_m^* as a function of the SIR threshold Θ. The network capacity

$$\lambda_{\mathrm{C}} = p_m^*(1-p_m^*)\left(1-\frac{p_m^*}{1+1/\Theta}\right)e^{-p_m^*/\sigma} \tag{19}$$

is shown in Fig. 9(b). Generally, the network capacity λ_{C} is achieved at a small $p_m \leq 0.4$ for all practical path loss exponents α [Fig. 9(a)]. Moreover, $\lambda_{\mathrm{C}}/p_m^* \in [0.35, 0.45]$, i.e., even if the ALOHA network operates in the capacity-optimal manner, only 40% transmission attempts will succeed.

B. Impact of the Correlations in ALOHA Networks

Since ALOHA networks usually do not operate in saturation, it is not appropriate to assume that $p_{\mathrm{b}}(k,i) \equiv 1$ and ignore the correlation between n_i and its interferer n_k. As shown in Fig. 10(a) ($\lambda = 0.1$), there is indeed a huge gap between

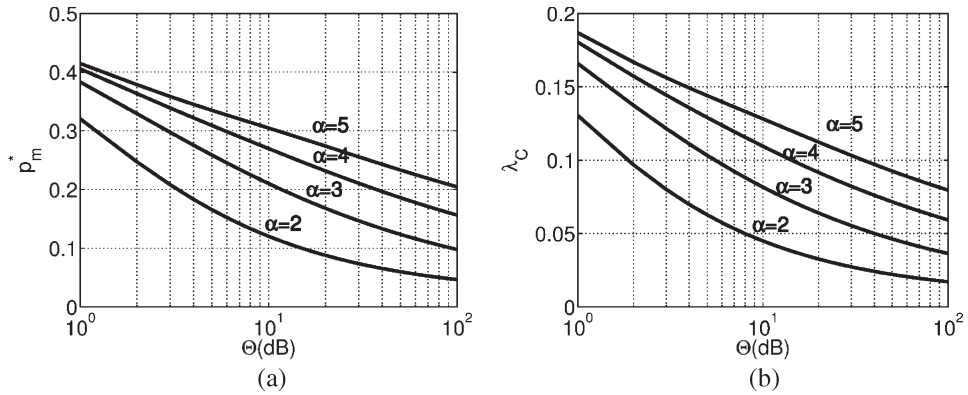

Fig. 9. Capacity of ALOHA line networks. (a) Optimal p_m^* to achieve the capacity. (b) Network capacity $\lambda_{\rm C}$.

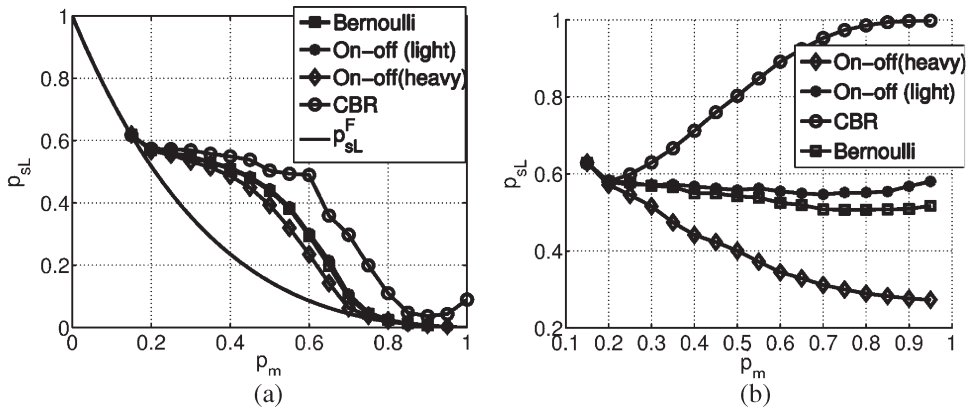

Fig. 10. Realistic channel performance in ALOHA networks with $\lambda = 0.1$, $\Theta = 10$, and $\alpha = 4$. (a) Independent flows. (b) Correlated flows.

the analytical worst channel quality $p_{\rm sL}^{\rm F}$ (15) in the saturated state and the simulated $p_{\rm sL}$ in the nonsaturated state. In fact, $p_{\rm b}(k,i) \to 1$ only if the traffic intensity $\rho = \lambda/(p_m p_{\rm sL})$ is close to one, which takes place when p_m is too small or too big. In the former case, the packets are held for a long time, so the buffer occupancy increases. In the latter case, more nodes transmit simultaneously to cause high interference and low success probability $p_{\rm sL}$. Consistently, the analytical $p_{\rm sL}^{\rm F}$ is tight in these two cases, e.g., $p_m < 0.2$ and $p_m > 0.8$. Other than that, the channel quality $p_{\rm sL}$ is much better than in the saturated state. For example, for CBR traffic, $p_{\rm sL} \in [0.5, 0.6]$ is almost unchanged with $p_m \in (0.2, 0.6)$, while the calculated $p_{\rm sL}^{\rm F}$ sharply decays from 0.5 to 0.1. Apparently, simply assuming $p_{\rm b}(k,i) \equiv 1$ substantially underestimates the channel quality.

Traffic statistics play an important role in affecting $p_{\rm b}(k,i)$. Like in TDMA, the impact of traffic correlation overshadows that of traffic burstiness. Therefore, the difference in $p_{\rm sL}$ between bursty and smooth traffic under the independent traffic flows [Fig. 10(a)] is less visible than under the correlated flows [Fig. 10(b)]. Moreover, for CBR traffic with correlated arrivals, it is counterintuitive that the channel quality $p_{\rm sL}$ does not decrease with an increasing p_m, as expected. Instead, $\partial p_{\rm sL}/\partial p_m > 0$, and $p_{\rm sL}$ converges to one [Fig. 10(b)]. This counterintuitive phenomenon occurs only with the CBR traffic. For bursty traffic, the increase of p_m does not enhance $p_{\rm sL}$. However, for Bernoulli and light bursty ON–OFF traffic, $\partial p_{\rm sL}/\partial p_m \approx 0$, so $p_{\rm sL}$ is less sensitive to p_m. It remains between 0.5 and 0.6 as p_m increases from 0.2 to 1. The only traffic model that follows the rule $\partial p_{\rm sL}/\partial p_m < 0$ as in the independent traffic flows is the heavy bursty ON–OFF traffic. Therefore, if the transmissions are random, the more bursty the traffic flow, the less beneficial the traffic correlation to the channel quality.

To explore why the traffic correlation leads to the surprising behavior of $p_{\rm sL}$ for the CBR traffic, recall that the probability $p_{\rm b}(k,i)$ reflects if n_k is busy, given that n_i is transmitting. In the case with completely correlated flows, there is a single source flow in the network, and the downstream nodes have packets only if their upstream nodes successfully sent them packets. Assume that n_1 is the source node, and consider $p_{\rm b}(k,1)$. Comparing $p_{\rm b}(k,1)$ with the unconditional busy probability ρ_k in Fig. 11(a), we arrived at the following findings.

1) A small $p_m = 0.15$ results in a high traffic intensity ρ_k, as in the conditional busy probability $p_{\rm b}(k,1)$, i.e., $\approx \rho_k \to 1$, and the two curves of ρ_k and $p_{\rm b}(k,1)$ almost completely overlap. The reason is that, in the heavy traffic case, the buffer is always nonempty, and the transmission is completely controlled by the MAC scheme, regardless of the traffic statistics.
2) As p_m increases to $p_m = 0.4$, the traffic intensity ρ_k decreases, and the busy period is shortened. Then, $p_{\rm b}(k,1) \le \rho_k < 1$, and the two curves of ρ_k and $p_{\rm b}(k,1)$ do not perfectly overlap, particularly at the nearest neighbors n_2 and n_3, which are more idle when n_1 is transmitting [with $p_{\rm b}(2,1) = 0.1$] than on average (with

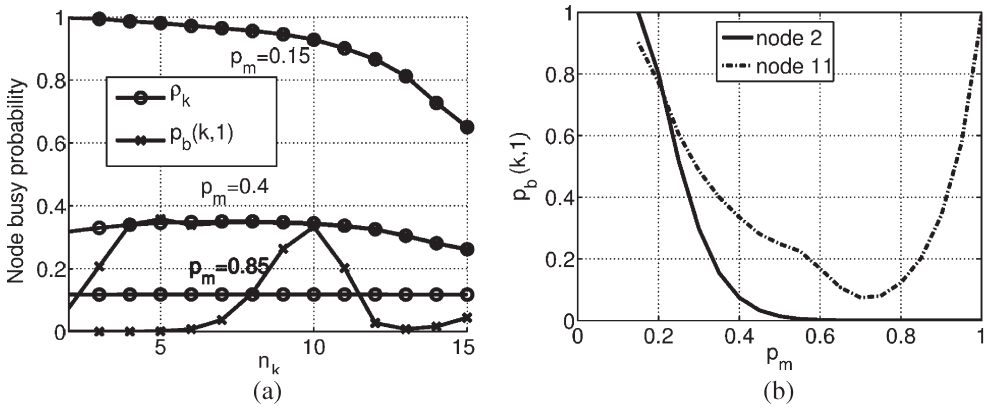

Fig. 11. Impact of traffic correlations on $p_{\rm b}(k,i)$ in ALOHA with CBR traffic and $\Theta = 10$, $\alpha = 4$. (a) Conditional busy probability $p_{\rm b}(k,1)$ given a transmit probability p_m for all nodes. (b) Conditional busy probability $p_{\rm b}(k,1)$ given a transmit probability p_m for special $k = 2$ and $k = 11$.

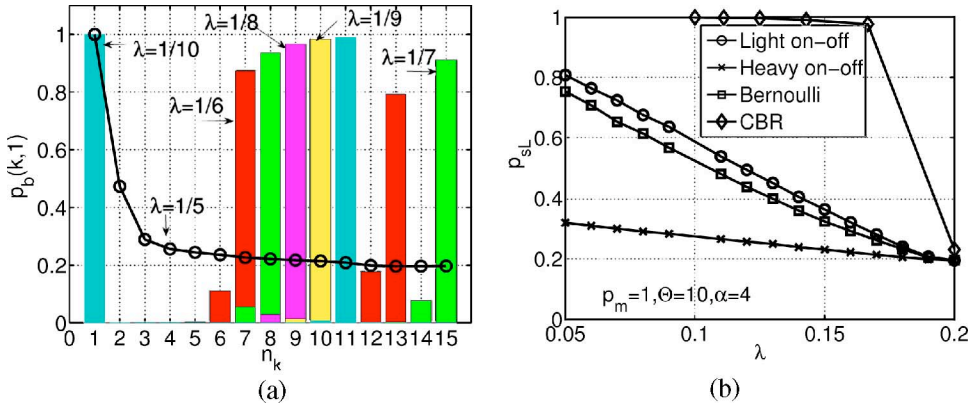

Fig. 12. Conditions on which ALOHA emulates TDMA to generate a natural spacing between the simultaneous transmitting nodes: 1) CBR traffic, 2) $p_m = 1$, and 3) arrival rate λ. ($\Theta = 10, \alpha = 4$). (a) Impact of the arrival rate λ on the conditional busy probability $p_{\rm b}(k,1)$. (b) Impact of traffic models on lower bound $p_{\rm sL}$ on the success probability.

$\rho_2 = 0.3$). The reason is that, in the mediate traffic case, the transmission is jointly controlled by both the MAC scheme and the traffic flows. The sequential transmission of packets from n_1 to n_2 to n_N starts to play a role in avoiding collisions caused by the simultaneous transmission of n_1 and n_2.

3) As p_m is close to one, e.g., $p_m = 0.85$, the transmission is mostly controlled by the traffic flows themselves rather than the MAC scheme, and $\rho_k \approx \lambda$ for all k's. The constant interarrival times at the source node silence most of its close neighbors when it is transmitting, i.e., $p_{\rm b}(k,1) \to 0$. On the other hand, the active nodes are all far away from n_1 with $p_{\rm b}(k,1) > \rho_k$ and form a spacing that is sufficiently wide to avoid severe interference.

It is no coincidence that at $\lambda = 0.1$, i.e., the interarrival time is ten slots, when n_1 is active, the most active node is n_{10}, which is almost ten hops away from n_1. In Fig. 11(b), we concentrate on two special nodes, namely, the nearest neighbor n_2 and the node n_{11}. The change of $p_{\rm b}(11,1)$ reflects how the MAC scheme and the traffic statistics jointly affect the network transmission order. At $p_m = 1$, the MAC scheme loses its influence, and the smoothness of CBR traffic is preserved. Then, the most powerful interferer n_2 becomes silent, while n_{11} becomes synchronous with n_1. A natural spacing between simultaneously transmitting nodes is formed, and ALOHA behaves like the m-phase TDMA with $m = 1/\lambda$.

It is interesting under which circumstances ALOHA can emulate TDMA. First, the arrivals at each node should be correlated. Second, the traffic should remain smooth in the network, which is guaranteed when $p_m \to 1$ and the traffic is CBR. Therefore, the bursty traffic like ON–OFF and Bernoulli cannot benefit from the increasing p_m [Fig. 10(b)]. However, the preservation of smoothness is not sufficient. Fig. 12(a) compares $p_{\rm b}(k,1)$ for different rates $\lambda = 1/m (m = 5, 6, \ldots, 10)$. Denote a virtual interference set of n_1 by $\tilde{\mathbb{I}}_1 = \{k | k = 1 + lm\} (l = 1, 2, \ldots)$, and recall that the potential interference set of n_1 in ALOHA is $\mathbb{I}_1 = \{k | k = 0, 1, 2, 3, \ldots\} \supset \tilde{\mathbb{I}}_1$. ALOHA emulates TDMA only if all the actual interferers belong to $\tilde{\mathbb{I}}_1$, i.e., $p_{\rm b}(k,1) \to 1$, for $k \in \tilde{\mathbb{I}}_1$, and $p_{\rm b}(k,1) \to 0$, for $k \notin \tilde{\mathbb{I}}_1$, which is true for $\lambda = 1/6, 1/7, 1/8, 1/9,$ and $1/10$. However, as shown in Fig. 12(a), for $\lambda = 1/5$, that rule no longer holds, and $p_{\rm b}(k,1) > 0$ for all $k \in \mathbb{I}_1$'s. Without the natural spacing, ALOHA cannot emulate TDMA, and the channel quality is sharply degenerated, as confirmed in Fig. 12(b). Therefore, the third condition is the rate constraint. From Fig. 12, the capacity can be read as $\lambda_{\rm C} = 0.2$. It is worth pointing out that the capacity under the correlated flows is greater than under the independent flows [Fig. 9(b)] ($\lambda_{\rm C} = 0.1$, for $\Theta = 10, \alpha = 4$).

More importantly, as long as the natural spacing is formed, the channel is very good with $p_{\rm sL} \geq 0.95$, even if the arrival rate

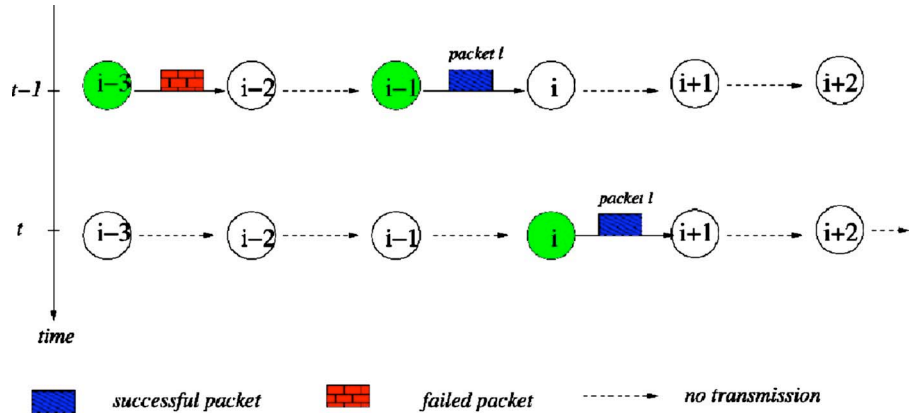

Fig. 13. Transmission order in ALOHA with $p_m = 1$ and dropping policy.

is close to $\lambda_{\rm C}$, for example, $\lambda = 1/6$ in Fig. 12(b). This property benefits not only the network throughput and capacity but also the end-to-end delay. Based on the queueing theory, if $p_{\rm sL}$ is unchanged, a large p_m implies a smaller access delay and, thus, a smaller overall waiting delay. Since the traffic correlation exists in most multihop networks, it is essential to exploit its advantages for QoS guarantees.

V. Emulation of TDMA for Non-CBR Traffic

The two critical conditions for ALOHA to emulate TDMA are the traffic correlation and the preservation of smoothness. The latter applies to only the CBR traffic. However, many applications are not as smooth as CBR. For non-CBR traffic, a simple solution to emulate TDMA is the use of traffic regulators, like leaky buckets, to smooth the bursty traffic flows at the source. Another solution is the employment of packet dropping.

Consider a basic packet dropping strategy, in which the failed packets are immediately discarded and successful packets are immediately forwarded by the relay node. Assume that there is a single source flow in the network. Then, queueing is avoided, and every node has, at most, one packet in the buffer. The transmission of n_i completely depends on n_{i-1} since n_i has packets to transmit at time t only if n_{i-1} successfully delivers a packet to it at time $t-1$. Therefore, prior to the study of the transmission of n_i at time t, we first observe the transmission of n_{i-1} at time $t-1$. At $t-1$, in order to guarantee the successful transmission from n_{i-1} to n_i, the following events must have occurred (see Fig. 13).

1) The desired receiver n_i did not transmit at $t-1$ since a node cannot transmit and receive at the same time. Therefore, n_{i+1} is idle at t.
2) n_{i-1} did not receive at $t-1$. Therefore, n_{i-1} is idle at t.
3) n_{i+1} did not transmit at $t-1$ since its transmission would interfere with that of n_{i-1} at n_i and fail the transmission at a very high probability as the most influential interferer of n_{i-1}. Therefore, its receiver n_{i+2} is idle at t.
4) n_{i-3} did not transmit for the same reason as 3). Therefore, n_{i-2} is idle at t.

In summary, when n_i transmits at t, at least, its four closest neighbors n_{i-2}, n_{i-1}, n_{i+1}, and n_{i+2} are idle, regardless of whether the traffic flow is bursty or smooth. For practical path loss exponents, simulation results show that the transmissions to n_{i-3} and n_{i+3} are hardly successful at $t-1$. Then, the nearest interferers of n_i at time t are n_{i-4} and n_{i+4}. Similarly, the interferers of n_{i-4} and n_{i+4} are at least four hops away from them. Accordingly, a natural spacing of $m = 4$ hops is formed with this simple dropping policy, and the corresponding network behaves like the m-phase TDMA. The advantages over TDMA are the following: 1) The spacing is naturally generated without the overhead of establishing and maintaining the frame structure; and 2) there is no access delay because $p_m = 1$.

Due to the similarity with TDMA, the performance of such networks can be derived in a similar way as in TDMA. For the case of correlated flows, n_1 is the only source generating a CBR flow of rate λ. The failed packets are discarded with probability $1 - p_{s,i}$. Then, the arrival rate at n_i is

$$\lambda_i = \lambda \prod_{k=1}^{i-1} p_{s,k} \geq \lambda p_{\rm sL}^{i-1}. \tag{20}$$

Since there is no access delay and no packet accumulation, the traffic intensity is $\rho_k = \lambda_k / p_{s,k}$, which is m times less than in TDMA. That is why the resulting $p_{\rm sL}$ is better than in TDMA, as shown in the following. Due to the nonhomogeneous traffic loads, the worst channel quality $p_{\rm sL}$ occurs at n_{m+1}. By plugging ρ_k into (6), we have

$$\begin{aligned} p_{\rm sL} &\approx \prod_{l \in \mathbb{J}} \left(1 - \frac{\lambda_l}{p_{\rm sL}(1 + l^\alpha/\Theta)}\right) \\ &\approx 1 - \frac{\lambda}{p_{\rm sL}} \left(\frac{1}{1 + m^\alpha/\Theta} + p_{\rm sL}^m \sum_{k=1}^{\infty} \frac{p_{\rm sL}^{km}}{1 + (km)^\alpha/\Theta}\right) \\ &\approx 1 - \frac{\lambda}{p_{\rm sL}} \left(\frac{1}{1 + m^\alpha/\Theta} + \frac{p_{\rm sL}^{2m}}{1 + m^\alpha/\Theta}\right) \\ &= 1 - \frac{\lambda\beta}{p_{\rm sL}} \left(1 + p_{\rm sL}^{2m}\right), \qquad \beta \triangleq \frac{1}{1 + m^\alpha/\Theta} \end{aligned} \tag{21}$$

where $\mathbb{J} = \{m+1\} \bigcup \{lm - 1\}_{l=1}^{\infty}$, and $\lambda_l = \lambda$ if $l = m+1$, and $\lambda_l = \lambda p_{\rm sL}^{(l+1)m}$ if $l \in \{lm-1\}_{l=1}^{\infty}$. The term with the

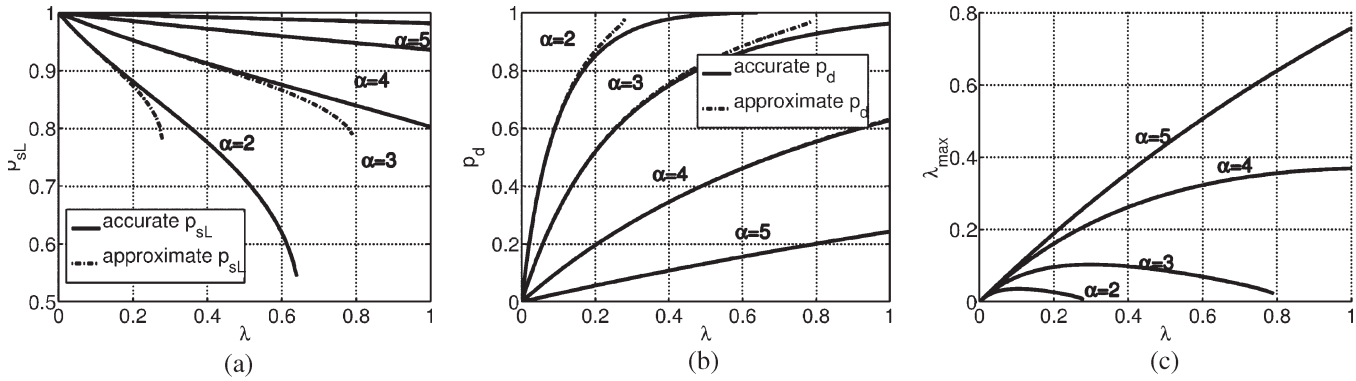

Fig. 14. Network performance of ALOHA with dropping strategy and $\Theta = 10$. (a) Channel quality $p_{\rm sL}$. (b) Packet dropping probability $p_{\rm d}$. (c) Network throughput $\lambda_{\max}$.

infinite sum is replaced by $\beta p_{\rm sL}^{2m}$ with a small error. Then, $p_{\rm sL}$ is solved as a root to the following polynomial:

$$f(x) = bx^{2m} + x^2 - x + b, \qquad \text{where} \quad b \triangleq \lambda\beta. \tag{22}$$

In order to obtain an explicit expression, we use the second-order Taylor expansion to yield a quadratic equation. Since $f(1) = 2b$, $f'(1) = 8b + 1$, and $f''(1) = 56b + 2$

$$p_{\rm sL} = \frac{1 + 48b + \sqrt{1 + 8b - 160b^2}}{2(1 + 28b)}. \tag{23}$$

For small λ, Fig. 14(a) shows that $p_{\rm sL}(\lambda)$ is linearly decreasing. The end-to-end dropping probability is upper bounded by $p_{\rm d} \leq 1 - p_{\rm sL}^N$, which is almost linear with λ for $\alpha \geq 4$ [Fig. 14(b)]. Note that due to packet dropping, there is no stability problem. The network throughput, based on the fundamental definition, is the number of packets that can be successfully transmitted to the destination, i.e.,

$$\lambda_{\max} = \lambda(1 - p_{\rm d}) \geq \lambda p_{\rm sL}^N \tag{24}$$

which is shown in Fig. 14(c). Since $m = 4$ is predetermined by the dropping policy, the network capacity is $\lambda_{\rm C} = \lambda_{\max}$.

Dropping packets en route reduces the reliability. However, this problem can be resolved by introducing redundancy. For instance, by using erasure correcting codes [27], more packets will be injected into the source node such that the destination node can recover the data, even if a fraction of the packets is lost. In Fig. 14(c), if a traffic flow of higher rate $\lambda = 0.3$ with 50% redundancy is injected, a throughput of $\lambda_{\max} = 0.2$ is guaranteed for $\alpha = 4$, and $\Theta = 10$. In TDMA, the highest arrival rate allowed is $\lambda_{\max} = 0.2$, while in this case, the throughput is enhanced to $\lambda_{\max} > 0.3$ when $\lambda \to 1$.

Meanwhile, the channel quality $p_{\rm sL}$ is also improved. For instance, at rate $\lambda = 0.3$, the channel is almost perfect with $p_{\rm sL} > 0.95$ [Fig. 14(a)], while in TDMA, at $\lambda_{\max} = 0.2$, the channel quality is $p_{\rm sL} < 0.9$ (Fig. 5). Since good channels cause short delays, the dropping strategy is more desirable, given that many applications can tolerate a small part of packet loss but are delay-sensitive. Furthermore, it is more energy efficient to discard outdated packets as early as possible than to keep retransmitting them since they will be dropped at the destination due to the expiration. Overall, it is beneficial to drop a small fraction of packets to save energy, reduce the end-to-end delay, improve the channels, and enhance the throughput.

VI. Conclusion

In this paper, we investigate three types of correlations in wireless multihop networks, namely, the autocorrelation in the channel quality $p_{\rm sL}$, the cross correlation between $p_{\rm sL}$ and the arrival rate λ, and the traffic correlation. Their impact is reflected through the node busy probability of the interferers. In TDMA networks, due to the spacing between the transmitter and the interferers, the traffic correlation can be ignored, and explicit expressions of the channel quality $p_{\rm sL}$, the network throughput $\lambda_{\max}$, and capacity $\lambda_{\rm C}$ are available. The statistical traffic parameters like burstiness are not as significant as the deterministic parameter, such as the arrival rate, in affecting the channel performance.

In ALOHA networks, the statistical traffic parameters become dominant, particularly the traffic correlation. We derive the throughput and capacity for the independent traffic flows. The network behaves differently under the correlated flows. In [26], it is found that if the error-prone wireless channel is characterized by a Bernoulli process with fixed success probability $p_{\rm s}$, a CBR flow is transformed to an ON–OFF flow, and the smoothness is destroyed. However, in interference-limited networks with Rayleigh fading channels, the smoothness can be preserved, even though the success probability is time varying. In other words, interference helps to preserve traffic smoothness. This surprising phenomenon is caused by the traffic correlation that makes ALOHA emulate TDMA by naturally forming a spacing between the transmitting nodes. Since the natural spacing does not require the overhead to establish and maintain the frame structure, the resulting performance is better than the TDMA in terms of capacity and delay. Therefore, ALOHA with $p_m = 1$ may be the best multihop MAC scheme possible when the original traffic flows are CBR and the arrivals in the network are closely correlated.

Our analysis also explains the design principle of fast-forward MAC for multihop networks, which aims to prevent the sender from consecutively transmitting before the previous packet has traveled beyond the interference range [11], [12].

Due to the traffic correlation, n_i knows that its neighbor n_{i+1} will certainly compete for a transmission opportunity in the following time slot after n_i succeeded in transmitting a packet. Then, n_i could withhold its transmission and let n_j transmit, which not only avoids collision but also decreases delay jitter. For bursty traffic, the MAC scheme could be jointly designed with traffic regulators to smooth traffic flows before injecting them into the network. If the analysis is extended to 2-D networks (regular or random) in which there are multiple routes and traffic multiplexing, then it could provide insight on the design of cross-layer protocol architecture involving MAC, routing and transport layer [12], or load balancing [28]. The most important advantage of correlations is the improvement of the network throughput and channel qualities and the reduction of the end-to-end delay and energy consumption.

REFERENCES

[1] B. Shrader, M. Sanchez, and T. C. Giles, "Throughput-delay analysis of conflict-free scheduling in multihop *ad-hoc* networks," in *Proc. 3rd Swedish Workshop Wireless Ad-Hoc Netw.*, May 2003.

[2] S. Toumpis and A. Goldsmith, "Performance, optimization, and cross-layer design of media access protocols for wireless *ad hoc* networks," in *Proc. IEEE ICC*, May 2003, vol. 3, pp. 2234–2240.

[3] M. Zorzi, "On the analytical computation of the interference statistics with applications to the performance evaluation of mobile radio systems," *IEEE Trans. Commun.*, vol. 45, no. 1, pp. 103–109, Jan. 1997.

[4] R. Mathar and J. Mattfeldt, "On the distribution of cumulated interference power in Rayleigh fading channels," *Wireless Netw.*, vol. 1, no. 1, pp. 31–36, Feb. 1995.

[5] M. Haenggi, "On the local throughput of large interference-limited wireless networks," in *Proc. 39th Annu. CISS*, Baltimore, MD, Mar. 2005.

[6] C. Knessl, "An explicit solution to a tandem queueing model," *Queueing Syst.*, vol. 30, no. 3/4, pp. 261–272, 1998.

[7] S. Kumar, V. S. Raghavan, and J. Deng, "Medium access control protocols for *ad hoc* wireless networks: A survey," *Elsevier Ad Hoc Netw. J.*, 2004.

[8] M. Sidi, "Tandem packet-radio queueing systems," *IEEE Trans. Commun.*, vol. COM-35, no. 2, pp. 246–248, Feb. 1987.

[9] R. Nelson and L. Kleinrock, "Spatial TDMA: A collision-free multihop channel access protocol," *IEEE Trans. Commun.*, vol. COM-33, no. 9, pp. 934–944, Sep. 1985.

[10] N. Abramson, "The ALOHA system—Another alternative for computer communications," in *Proc. Fall Joint Comput. Conf., AFIPS*, 1970, vol. 37, pp. 281–285.

[11] Z. Ye, D. Berger, P. Sinha, S. Krishnamurthy, M. Faloutsos, and S. K. Tripathi, "Alleviating MAC layer self-contention in *ad-hoc* networks," in *Proc. ACM Mobicom*, Sep. 2003.

[12] L. Bononi and M. D. Felice, "Performance analysis of cross-layered multipath routing and MAC layer solutions for multi-hop *ad hoc* networks," in *Proc. ACM MobiWAC*, Torremolinos, Spain, Oct. 2006, pp. 190–197.

[13] P. Karn, "MACA—A new channel access method for packet radio," in *Proc. ARRL/CRRL Amateur Radio 9th Comput. Netw. Conf.*, Sep. 1990, pp. 134–140.

[14] Z. J. Haas and J. Deng, "Dual busy tone multiple access (DBTMA)—A multiple access control scheme for *ad hoc* networks," *IEEE Trans. Commun.*, vol. 50, no. 6, pp. 975–985, Jun. 2002.

[15] J. Li, C. Blake, D. S. J. D. Couto, H. I. Lee, and R. Morris, "Capacity of *ad hoc* wireless networks," in *Proc. ACM MobiCom*, Rome, Italy, Jul. 2001, pp. 61–69.

[16] B. Tavli and W. B. Heinzelman, "MH-TRACE: Multihop time reservation using adaptive control for energy efficiency," *IEEE J. Sel. Areas Commun.*, vol. 22, no. 5, pp. 942–953, Jun. 2004.

[17] J. C. Fang and G. D. Kondyli, "A synchronous, reservation based medium access control protocol for multihop wireless networks," in *Proc. IEEE WCNC*, Mar. 2003, vol. 2, pp. 994–998.

[18] H. Zhai, J. Wang, and Y. Fang, "Distributed packet scheduling for multihop flows in *ad hoc* networks," in *Proc. IEEE WCNC*, Mar. 2004, vol. 2, pp. 1081–1086.

[19] V. Saligrama and D. Starobinski, "On the macroscopic effects of local interactions in multi-hop wireless networks," in *Proc. Int. Symp. Model. Optim. Mobile, Ad Hoc, Wireless Netw.*, 2006, pp. 1–8.

[20] A. Chockalingam, M. Zorzi, L. B. Milstein, and P. Venkataram, "Performance of a wireless access protocol on correlated Rayleigh-fading channels with capture," *IEEE Trans. Commun.*, vol. 46, no. 5, pp. 644–655, May 1998.

[21] J. C. Mogul, "Observing TCP dynamics in real networks," in *Proc. SIGCOMM Symp. Commun. Architectures Protocols*, 1992, pp. 305–317.

[22] N. Ryoki, K. Kawahara, T. Ikenaga, and Y. Oie, "Performance analysis of queue length distribution of tandem routers for QoS measurement," in *Proc. SAINT Workshops*, 2002, pp. 82–87.

[23] M. Xie and M. Haenggi, "Delay performance of different MAC schemes for multihop wireless networks," in *Proc. GLOBECOM*, Nov. 2005, pp. 3423–3427.

[24] M. M. Carvalho and J. J. Garcia-Luna-Aceves, "A scalable model for channel access protocols in multihop *ad hoc* networks," in *Proc. ACM MobiCom*, Sep. 2004, pp. 330–344.

[25] M. Haenggi, "Outage and throughput bounds for stochastic wireless networks," in *Proc. IEEE ISIT*, Adelaide, Australia, Sep. 2005, pp. 2070–2074.

[26] M. Xie and M. Haenggiin "Statistical delay analysis of TDMA and ALOHA in wireless multihop networks," 2006. Tech. Rep. [Online]. Available: http://www.nd.edu/~mhaenggi/pubs/xie06.pdf

[27] M. G. Luby, M. Mitzenmacher, M. A. Shokrollahi, and D. A. Spielman, "Efficient erasure correcting codes," *IEEE Trans. Inf. Theory*, vol. 47, no. 2, pp. 569–584, Feb. 2001.

[28] B. Ngo and S. Gordon, "Avoiding bottlenecks due to traffic aggregation at relay nodes in multi-hop wireless networks," in *Proc. Asia-Pac. Conf. Commun.*, Oct. 2005, pp. 769–773.

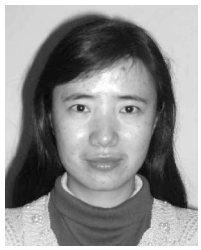

Min Xie received the B.S. and M.S. degrees in electrical engineering from Xidian University, Xi'an, China, in 1996 and 1999, respectively, the M.S. degree in electrical and computer engineering from the National University of Singapore, Singapore, in 2001, and the Ph.D. degree in electrical engineering from the University of Notre Dame, Notre Dame, IN, in 2007.

She was with the University of Notre Dame. She is currently a Research Associate with University College London, London, U.K. Her research interests include the design and analysis of media-access-control and scheduling schemes, QoS guarantees, and performance analysis of wireless networks.

Martin Haenggi (S'95–M'99–SM'04) received the Dipl. Ing. (M.Sc.) and Ph.D. degrees in electrical engineering from the Swiss Federal Institute of Technology (ETHZ), Zurich, Switzerland, in 1995 and 1999, respectively.

After a postdoctoral year with the Electronics Research Laboratory, University of California, Berkeley, he has been with the Department of Electrical Engineering, University of Notre Dame, Notre Dame, IN, since 2001, where he is currently an Associate Professor. His scientific interests include networking and wireless communications, with an emphasis on *ad hoc* and sensor networks.

Dr. Haenggi is a member of the Editorial Board of the *Elsevier Journal on Ad Hoc Networks*. He was the recipient of the ETH medal for both his M.Sc. and Ph.D. theses and also the CAREER Award from the U.S. National Science Foundation in 2005.